Available online at BCREC website: https://bcrec.id

Bulletin of Chemical Reaction Engineering & Catalysis, 16 (1) 2021, 136-147

Research Article

Physical-chemical Characterization of Nano-Zinc Oxide/Activated Carbon Composite for Phenol Removal from Aqueous Solution

Allwar Allwar*), Asih Setyani, Ulul Sugesti, Khusna Afifah Fauzani

Department of Chemistry, Faculty Mathematics and Natural Sciences, Universitas Islam Indonesia, Yogyakarta, 55584, Indonesia.

Received: 4th February 2021; Revised: 23rd March 2021; Accepted: 23rd March 2021
Available online: 25th March 2021; Published regularly: March 2021

Abstract

Oil palm shell was used as a precursor for preparation of activated carbon using different chemical activations (potassium hydroxide (KOH), zinc chloride ($ZNCl_2$), and phosphoric acid (H_3PO_4)). Each activated carbons (AC) was mixed with nano-zinc oxide to form a composite. From the gas sorption analyzer, it is showed that nitrogen adsorption isotherms show Type II for ZnO/AC-KOH and ZnO/AC-$ZnCl_2$ corresponding to the micro- and mesoporous structures, respectively. However, the nitrogen adsorption isotherm of ZnO/AC-H_3PO_4 exhibits the Type I with predominantly microporous structures. The SEM micrographs produced unsmooth surface and different pore sizes. The XRD patterns at 2θ of 25.06° and 26.75° were come from amorphous activated carbon. The peak intensity of ZnO was weak due to low concentration of zinc precursor. However, the ZnO of ZnO/AC-$ZnCl_2$ showed strongly peak intensity. The effectiveness of the composites was examined for phenol removal determined by UV-Vis Spectrophotometer method. The equilibrium adsorption follows the Langmuir and Freundlich models according to the best correlation coefficient (R^2). The kinetic model was only obtained for the pseudo-second-order with the best linearity of the correlation coefficient (R^2). The results of this study showed that the oil palm shell has a great potential for ZnO/AC with excellent adsorptive property.

Keywords: Oil palm shell; Activated carbon; Zinc oxide; Phenol; Langmuir and Freundlich

How to Cite: A. Allwar, A. Setyani, U. Sugesti, K.A. Fauzani (2021). Physical-chemical Characterization of Nano-Zinc Oxide/Activated Carbon Composite for Phenol Removal from Aqueous Solution. *Bulletin of Chemical Reaction Engineering & Catalysis*, 16(1), 136-147 (doi:10.9767/bcrec.16.1.10282.136-147)

Permalink/DOI: https://doi.org/10.9767/bcrec.16.1.10282.136-147

1. Introduction

Phenol and its derivate are the most common hazard chemicals even at low concentration in wastewater [1,2]. Phenolic compounds can be easily obtained in the effluent of wastewater coming from the petrochemical industries, textile, pesticides, petroleum refineries, resin industries, dye synthesis, pharmaceutical industries [3,4]. Their properties are highly corrosive that can severe the human being and living things. Some methods have been applied to remove or recovery of aquatic environment including the adsorption, ion exchange, precipitation, oxidation gas and steam stripping. Among them, adsorption using porous materials is the most popular method because of its excellent pore structures and highly adsorption capacity. Porous material is class of solid materials with low density, high surface area and a range of novel properties in physical and chemical fields. The pore can be clarified into micropore (pore diameter <2 nm), mesopore (pore diameter 2–50

* Corresponding Author.
Email: allwar@uii.ac.id (A. Allwar)

nm) and macropore (pore diameter >50 nm). Porous material has been intensively studied in the design and synthesis, characterization and property evaluation. The designing of porous material with metal oxide to form composite results advantages properties such as thermal stability, improving of physical and chemical properties, censors, catalyst and separations. Previous study reported that the porous activated carbon with zinc oxide is one of the most popular adsorbents for removal of dyes in aqueous solution [5].

Porous activated carbon is an excellent material having high surface area, pore volume, pore size distribution and functional groups. It can be prepared from many types of biomass such as oil palm shell, coconut shell, bagasse, bone using physical or chemical processes. However, the activated carbon itself still have less structures and complex physiochemical properties such as poor selective adsorption, low thermal stability, kinetic and non-equilibrium adsorption [6]. Due to high requirement of activated carbon, scientists have to find the new alternative precursor and improve their property. Combination of activated carbon with nanoparticle metal oxide is one of popular methods to produce a better sorption property. Nanoparticle such as zinc oxide (ZnO) is widely used as adsorbent in the wastewater treatments. It has excellent properties such as photo-catalytic, antibacterial and capacitor materials which are non-toxic and thermal stability. The growing of ZnO onto activated carbon as metal carbon matrix reinforcement has been intensively studied to improve the composite's performance including surface area and adsorptive capacity.

Previous studies reported that the mixture of ZnO and activated carbon have been applied in many applications as adsorbent for removal of heavy metal ion, capacitor and catalyst [7,8]. Development of activated carbon to find an excellent property will be a great challenge in the future including its pore structure, method and raw material type. Preparation of ZnO/activated carbon with different chemical activations and modified zinc oxide has been attracted to develop including the properties and application.

The objectives of this work are to synthesize and characterize of zinc oxide/activated carbon (ZnO/AC) composites. Activated carbon and ZinO/activated carbon were characterized by the Fourier transform infrared (FTIR) spectroscopy (Perkin Elmer Spectrum Version 10.5.1), Gas sorption analyzer (GSA) (Quanthachrome), Scanning electron microscope with Energy dispersive X-ray (SEM-EDX) analysis (JEOL JED-2300), X-ray diffraction (XRD) method (Bruker D2 Phaset Gen). The graphite furnace is from (Nabertherm). Adsorption capacity of phenol was evaluated at various parameters such as pH solution, concentration, adsorbent dosage and contact time using UV-Visible spectrophotometer (Hitachi UH5300) [9].

2. Material and Methods

2.1 Materials

Biomass of oil palm shell was obtained from open area at around palm oil industry. All chemicals such as potassium hydroxide (KOH), phosphorous acid (H_3PO_4), zinc chloride ($ZnCl_2$), phenol, chloride acid (HCl), zinc oxide nanoparticle (ZnO), and nitric acid (HNO_3) were purchased from Merck with analytical grade and used without further purification.

2.2 Preparation of Activated Carbon

Oil palm shell was washed with hot distilled water to reduce oil and dirt contents and dried in the oven at 110 °C for 24 h. The dried shell was grounded and sieved to particle size in the range of 0.1–0.5mm. Approximately, 250 g of shell was impregnated with each of 500 ml of each 20% H_3PO_4, $ZnCl_2$ or KOH solution and refluxed at 85 °C for 6 h [10,11]. To reduce chemical content, samples were washed with distilled water, neutralized to pH 6-7 using acid or based solution and dried in oven at 110 °C for 24 h. Each of samples was carbonized into stainless steel reactor to 500 °C for 3 h with heating rate of 5 °C.min^{-1}. During carbonization, purified nitrogen gas was flowed into the reactor at a constant rate of 200 cm^3 min^{-1}. The resulted carbonization was washed with distilled water to remove ash content. Dried samples were and kept in desiccator as activated carbon of AC-KOH, AC-H_3PO_4, and AC-$ZnCl_2$.

2.3 Preparation of Activated Carbon/ZnO

Prior to preparation of composite, activated carbons (AC-KOH, AC-H_3PO_4 and AC-$ZnCl_2$) were modified with 3 M HNO_3 solution to remove metal contents and to activate functional group which are anchored on the carbon. Modified activated carbons were dried in an oven at 110 °C for 24 h. Approximately, 20 g of nanoparticle zinc oxide was loaded to 100 g each of activated carbon in the hydrothermal reactor and continued into graphite furnace. The mixtures were added with the deionized water and ethanol (2:1) and strongly shaken for 2 h. Tem-

perature of graphite furnace was gradually increased to 150 °C for 4 h. After cooling down, the composites were dried and labeled as ZnO/AC-composite consisting of ZnO/AC-KOH, ZnO/AC-H_3PO_4 and ZnO/AC-$ZnCl_2$.

2.4 Characterization of Composites

Characterization of ZnO/AC-composite was identified by nitrogen adsorption isotherms at 77 K. The BET surface area was obtained at relative pressure (P/Po) in the range of 0.05–0.3. Total pore volume was obtained at maximum P/Po=0.99. The presences of functional groups on the composite's surface were evaluated by the Fourier Transform Infrared Spectroscopy (FTIR) at wavelength in the range of 4000–400 cm^{-1} [12]. Surface morphology and elemental analysis were carried out by the Scanning Electron Microscopy-Energy and Dispersive X-Ray (SEM-EDX). The crystalline and unit cell dimension were studied by the X-ray powder diffraction (XRD) [13].

2.5 Removal of Phenol

The amount of phenol removal onto ZnO/AC-composite was evaluated using batch method at room temperature. The experiment data was obtained from equilibrium adsorption isotherm at varying adsorption parameters such as concentration, pH, adsorbents weight and contact time. The sorption rate of phenol was determined by the UV-Visible spectrophotometry at wave length of 270–274 nm. The percentage adsorption (%R) was calculated as presented in Eq. (1).

$$\%R = \frac{C_0 - C_e}{C_0} \times 100 \quad (1)$$

The Langmuir and Freundlich isotherm models were applied to evaluate the equilibrium adsorption. The Langmuir is presumed as monolayer adsorption relating to the specific homogeneous surface. The Freundlich is assumed as multilayer adsorption occurring on the heterogeneous surface.

3. Result and Discussion

3.1 Nitrogen Adsorption Isotherm Analysis

The nitrogen adsorption isotherms are displayed in Figure 1. The nitrogen isotherms of ZnO/AC-KOH and ZnO/AC-$ZnCl_2$ show similar plots exhibiting type II isotherms corresponding to the presence of micro- and mesoporous structures. Compared with the ZnO/AC-H_3PO_4, nitrogen isotherm plot tends to show type I isotherm with predominantly microporous structures. The resulted study indicated that the effect of phosphoric acid showed that an increasing the formation of micropore compared to the potassium hydroxide and zinc chloride. Textural characteristic of ZnO/AC-composite is shown in Table 1. The results of BET surface area were not satisfactory. The experiment data showed that the desorption isotherm do not coincide with the adsorption isotherm creating

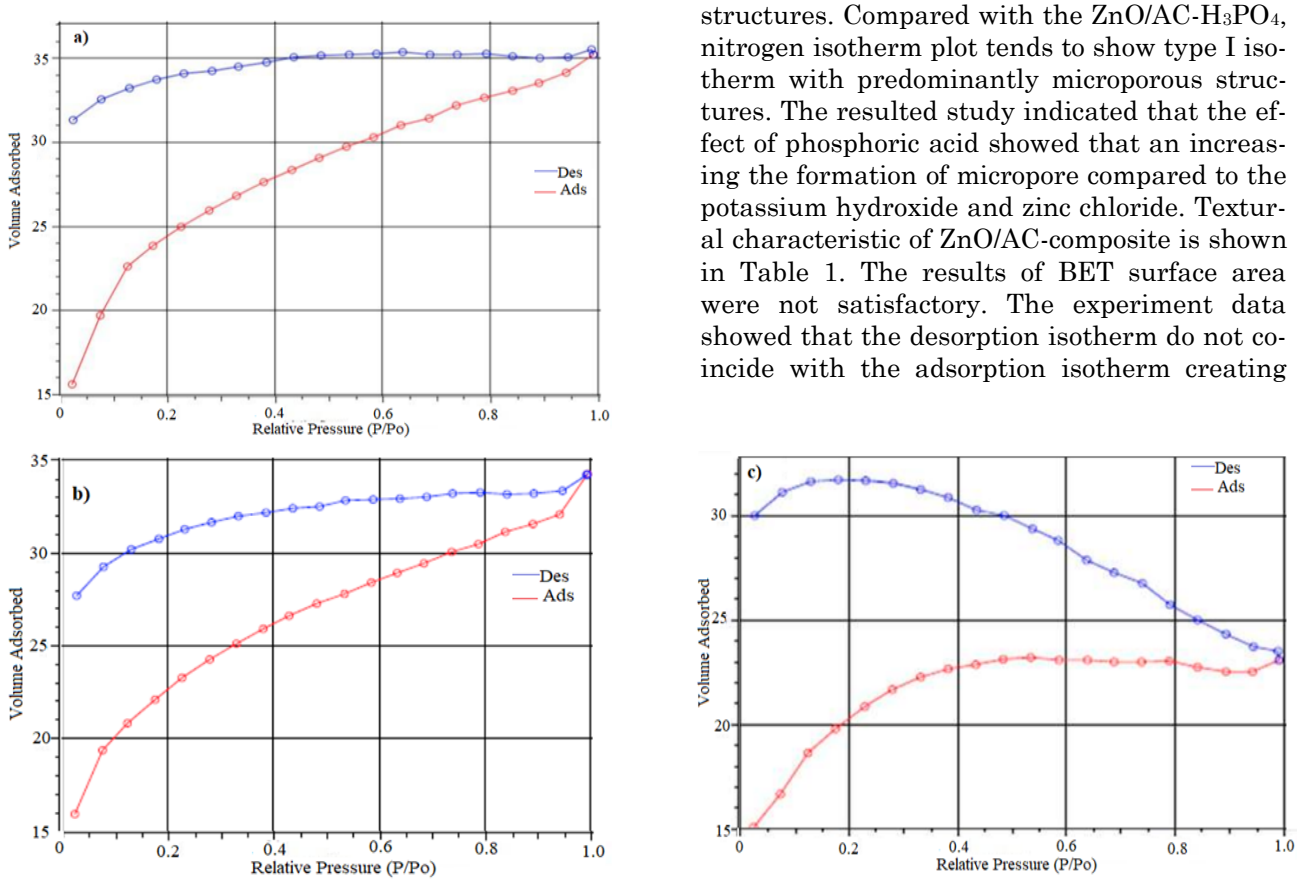

Figure 1. Nitrogen adsorption of ZnO/AC-composite: (a) ZnO/AC-KOH, (b) ZnO/AC-$ZnCl_2$, and (c) ZnO/AC-H_3PO_4.

wide hysteresis loop. In case of desorption process some of porosity could be broken that closed the porosity. As a result, desorption process was much slower than adsorption process due to poor porosity [14]. The maximal surface area was obtained at ZnO/AC-KOH. Average pore sizes of the composites were presence in the range of 1.02–1.31 nm corresponding to the predominantly microporous structure. It can be seen that the effects of activating agents have influenced the formation of pore structures. The activating agents KOH and H_3PO_4 might support to bond cleavage reaction of precursor and rearrangement to form the pore structure. Therefore, zinc chloride has thermal stability which was assumed to improve the performance of pore structures. It is well known that surface and pore size play important roles to support the adsorption of phenol process [15].

3.2 Functional Group Analysis

The presences of functional groups of activated carbon and ZnO/AC-composite were studied through the FTIR spectra as displayed in Figure 2. The weak bands at around 3749–3671 cm^{-1} are assigned as O–H stretching vibration group from H_2O. The bands at 1697

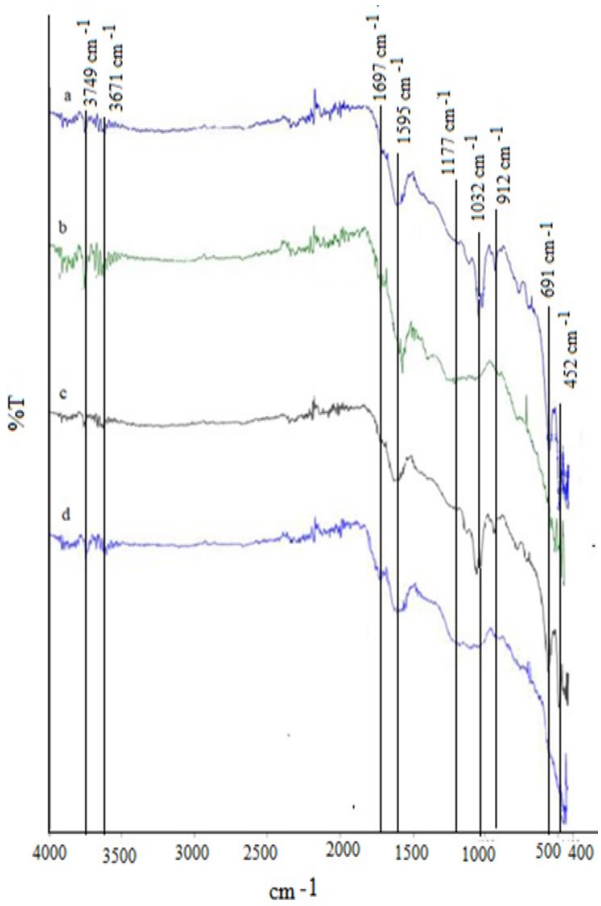

Figure 2. The FTIR spectra of (a) activated carbon, (b) ZnO/AC-KOH, (c) ZnO/AC-$ZnCl_2$, (d) ZnO/AC-H_3PO_4.

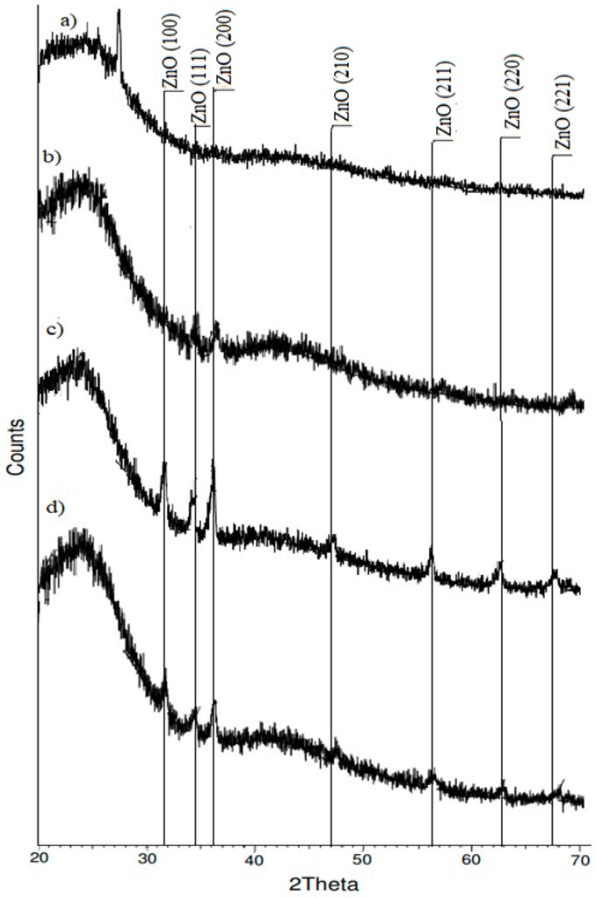

Figure 3. XRD spectrum (a) activated carbon; (b) Zn/AC-KOH (c) Zn/AC-$ZnCl_2$ (d) Zn/AC-H_3PO_4.

Table 1. Textural characterization of nano-ZnO/ACs.

Activation	BET Surface area ($m^2.g^{-1}$)	*t*-plot		Total pore volume (p/po= 0.99) ($cm^3.g^{-1}$)	Average pore size (nm)
		Micropores Surface area ($cm^2.g^{-1}$)	External surface area ($m^2.g^{-1}$)		
ZnO/AC-KOH	82.1	42.1	40.0	0.05	1.28
ZnO/AC-$ZnCl_2$	76.2	36.2	40.0	0.05	1.31
ZnO/AC-H_3PO_4	69.9	42.5	27.4	0.04	1.02

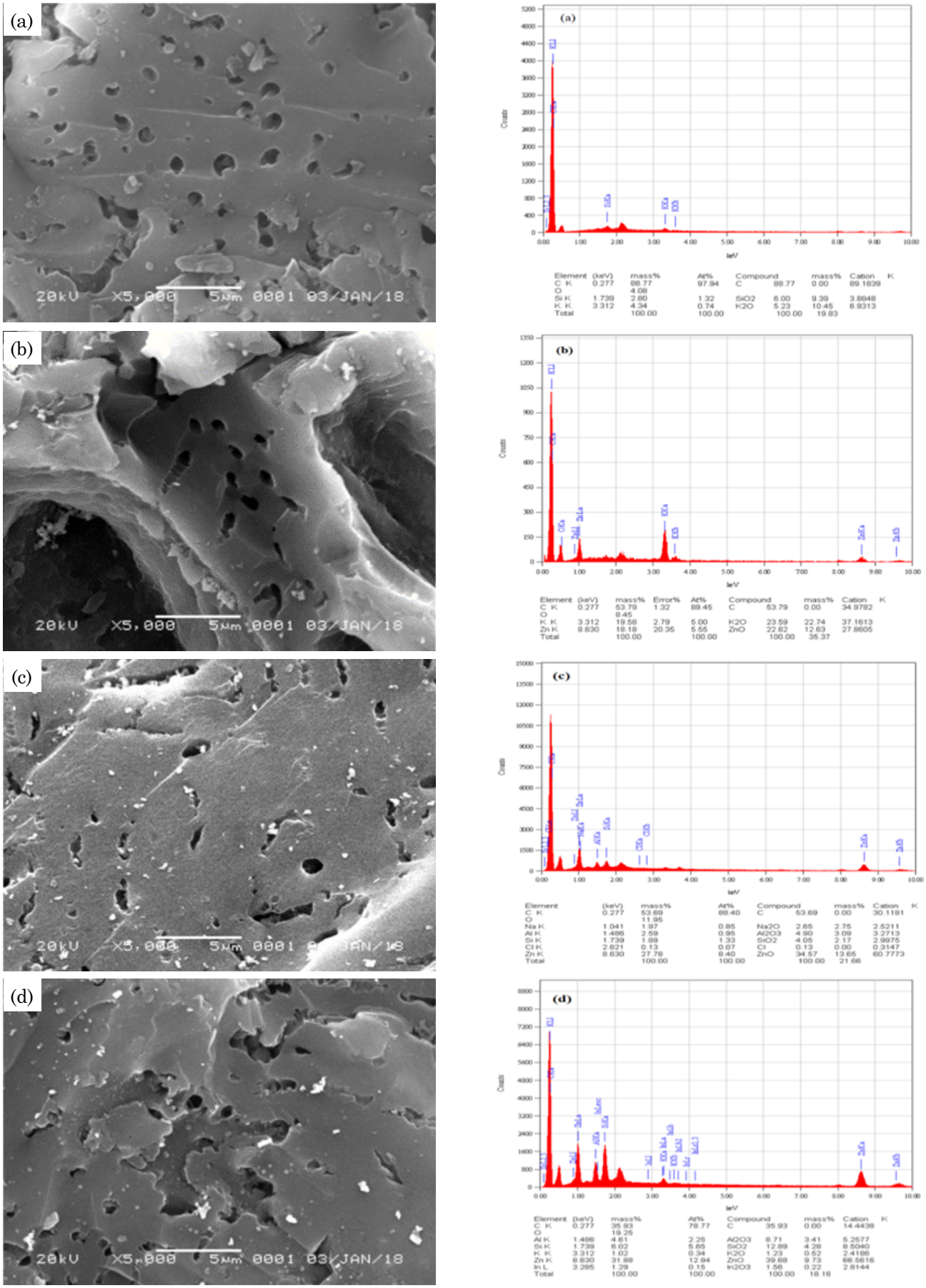

Figure 4. Surface morphology (a) activated carbon; (b) ZnO/AC-KOH; (c) ZnO/AC-$ZnCl_2$; (d) ZnO/AC-H_3PO_4.

cm^{-1} and 1595 cm^{-1} are assigned to C=O stretching vibration in carboxylic group and C=C stretching vibration in aromatic ring, respectively. The bands in the range of 1177–1032 cm^{-1} are ascribed to C–O stretching vibrations. of cellulose or hemicellulose from raw material. It can be seen that the band at 1023 cm^{-1} is only obtained on the activated carbon and ZnO/$ZnCl_2$ which indicate to have more C–O functional groups. The bands at around 691 cm^{-1} are related to C–H out-of-plane deformation vibration of C–H groups located at the edges of aromatic rings. It was assumed that the presence of functional groups on the surface is from the conversion of cellulose supported with chemical activation into activated carbon during pyrolysis process. The band in the range 452 cm^{-1} are assigned to Zn–O–C bond stretching vibration.

3.3 X-ray Diffraction Analysis

The XRD patterns of activated carbon and ZnO/AC-composite were obtained at 2θ ranging from 20–70° as shown in Figure 3. The peak at 2θ= 25.06° and 26.75° proved the amorphous structures of activated carbon as displayed in Figure 3(a). The XRD patterns of composite ZnO/AC-composite were determined with the performance in the range of 2θ = 31.70° (100), 34.44° (111), 36.32° (200), 47.58° (210), 56.56° (211), 62.85° (220), and 67.96° (221). This result is closed to the JCPDS Card No. 89-1397 [16,17]. The formation of crystalline phase on the composites could be occurred during the heating process in the hydrothermal reactor. However, the degrees of crystalline phases of all composites are weak due to the low concentration of zinc precursor with ratio of activated carbon and zinc oxide (5:1). The effect of additional chemical activation could influence the crystalline phase of zinc oxide. The strong peak was only obtained at ZnO/AC-$ZnCl_2$ is indicative of high crystalline phase. This result was assumed that the presence of $ZnCl_2$ as the activating agent could accelerate the formation of crystalline phase.

3.4 SEM-EDX Analysis

SEM micrographs and the Energy Dispersive X-ray analysis (EDX) of elemental micro-

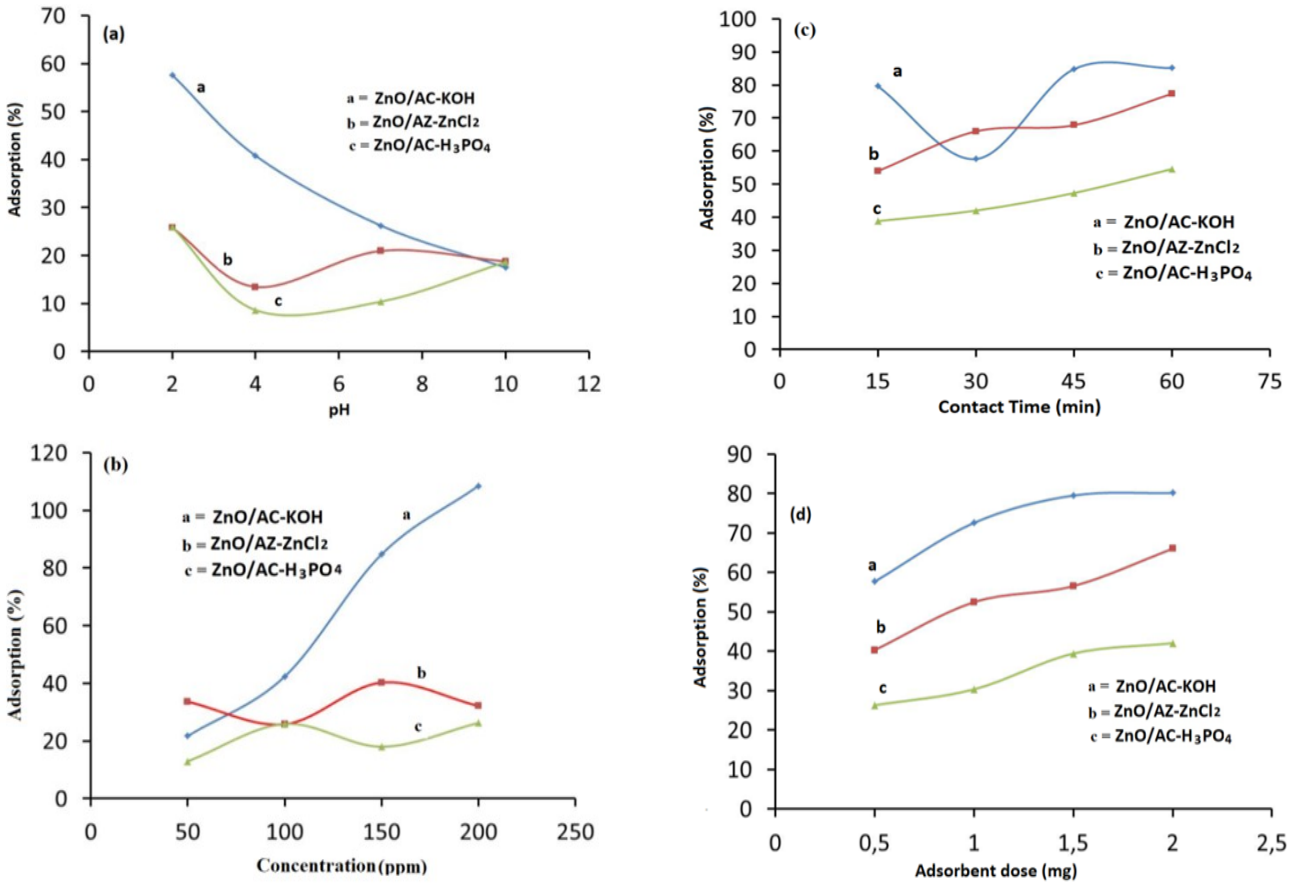

Figure 5. The curve of adsorption with different (a) pH, (b) concentration, (c) time and (d) weight adsorbent.

analysis of ZnO/AC-composite play important roles to study the exchanges of surface different chemical activations as shown in Figure 4. The surface of activated carbon and composites were clearly developed with unsmooth surface and disordered porous sizes. Comparison study showed that there were different feature between activated carbon and composite ZnO/activated carbon. The white color attached on the surface of activated carbon was assumed as zinc oxide that can be confirmed from the XRD result. The EDX analysis confirmed the elemental analysis of composites. The result showed that the ZnO/AC-KOH consists of 54% and 23% of carbon and zinc oxide, respectively; ZnO/AC-$ZnCl_2$ showed 54% and 18% for carbon and zinc oxide, respectively, and ZnO/AC-H_3PO_4 are 37% and 32% for carbon and zinc oxide, respectively. The amount of carbon decreased with increasing zinc content in the ZnO/AC-composite which might influence the degree of crystalline phase.

3.5 Effect of pH

The pH solution plays important roles in the adsorption process. The effect of pH solution on the phenol removal was carried out in the range of pH 2–10 as shown Figure 5(a). The maximum adsorption of phenol was obtained at pH= 2 or acidic condition and decreased as increasing pH solution. Adsorption of phenol could be happed by the transfer electron through H-bonding and aci based interaction [18,19]. In general, the adsorption capacity of phenol decreased with the increasing of pH solution, although adsorption capacity for ZnO/AC-H_3PO_4 and ZnO/AC-$ZnCl_2$ increase at pH 7. This study indicated that removal of phenol was found to be more suitable on the acid condition. The reason of this study showed that the surface of composite changed to be negative charge, and the phenol became a positive charge in acid solution. Interactions between composite and phenol showed favor electrostatic interactions in the acid condition leading strong adsorption. However, increasing of adsorption capacity phenol at pH 7 is the indication the surface of composite ZnO/AC-$ZnCl_2$ and ZnO/AC-H_3PO_4 changed to be a positive charge. This data was supported with previous research that the zero-point charge of ZnO was found at pH 6.25. This information exhibited that below pH 6.5 the surface charge is negative and above pH 6.5, it is positive. At the same reason, phenol was a weak acid with pKa = 9.98. It was assumed that at pKa < 9.98, phenol is positive charge and at pKa > 9.98, phenol dissociates to be negative charge [20]. In contrast, increasing pH solution showed that the surface composites are negative charge, and then the phenol produce negative charge, as a result to reduce the removal of phenol [21].

3.6 Kinetic Studies

Kinetics experiments were performed to study the adsorption behavior of phenol onto the composites. The equilibrium adsorption amount of phenol (q_e) per unit mass of adsorbent at time t (mg.g^{-1}) were calculated as following Eq. (2).

$$q_e = \frac{(C_0 - C_e)V}{m} \quad (2)$$

where V is the volume solution of phenol (L); C_0 and C_e the initial and remaining of phenol concentration in solution (mg.L^{-1}) at time t, respectively and m is the mass of the adsorbent (g).

The percentage of adsorption increased with the rise of concentration as shown in Figure 5(b). It can be seen that the sorption rate of phenol onto ZnO/AC-KOH sharply increased to maximum concentration, if it is compared to other composites. This reason can be explained that there are many phenolic compounds can be adsorbed onto activated carbon through the active sites of composite. However, the decreasing of adsorption process is the indicative of the insufficient pores that can be used to trap phenolic compounds into active sites of composite.

3.7 Effect of Contact Time

The effects of contact time on the extent of phenol removal onto ZnO/AC are shown in Figure 5(c). The amounts of phenol removal were evaluated from 15 to 60 min at room temperature. As the contact time increased, interaction between ZnO/AC-composite and phenol gave enough time to build reaction and provided a greater availability for the exchangeable sites in the adsorption process. The results show that percentages of phenol removal increased from initial contact time to reach maximum value at 60 min.

3.8 Effect of Adsorbent Weight

The effects of adsorbent weight on the phenol removal onto composites are displayed in Figure 5(d). It was clearly seen that percentage of phenol removal gradually increased with an increasing adsorbent weight. For each of composite showed that ZnO/AC-KOH showed the

highest percentage of phenol removal. However, the highest efficiency of phenol removal was obtained at weight adsorbent of 2 g. This reason was assumed that increasing weight adsorbent may increase the ability to adsorb more phenol as a result of increasing surface area. This phenomenon indicates that the composites were effective in the weight range of studied.

3.9 Adsorption Isotherm

Determination of equilibrium isotherm in adsorption process is one of the most important factors to study the behavior adsorption. In this study, two isotherm models, the Langmuir and Freundlich isotherm were introduced to investigate the interaction between adsorbate (phenol) and adsorbent (composite) in aqueous

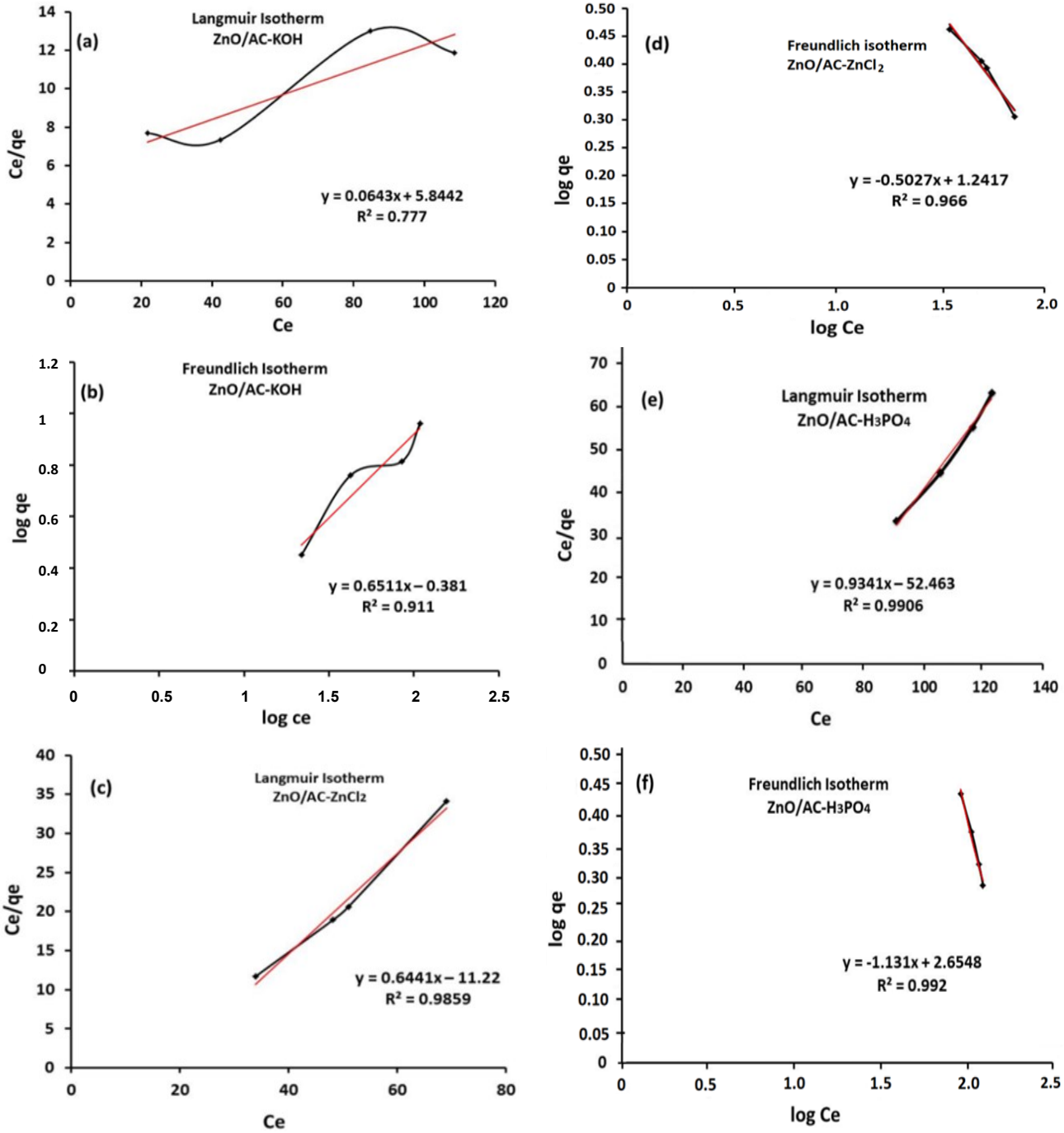

Figure 6. Langmuir and Freundlich isotherms of phenol onto composites: a) Langmuir isotherm with the ZnO/AC-KOH; b) Freundlich isotherm with the ZnO/AC-KOH; c) Langmuir isotherm with ZnO/AC-$ZnCl_2$; d) Freundlich isotherm with the ZnO/AC-$ZnCl_2$; e) Langmuir isotherm with the ZnO/AC-H_3PO_4; f) Freundlich isotherm with the ZnO/AC-H_3PO_4.

solution. The Langmuir isotherms model is usually used to describe monolayer with specific homogeneous sites on the surface [22]. The Langmuir isotherm data is calculated as the following Eq. (3).

$$\frac{C_e}{Q_e} = \frac{1}{K_L Q_m} + \frac{C_e}{Q_m} \quad (3)$$

where Q_e is the amount phenol adsorbed at equilibrium (mg.g^{-1}), C_e is the equilibrium concentration of phenol in solution (mg.L^{-1}), Q_m is the maximum adsorption capacity corresponding to complete monolayer coverage (mg.g^{-1}) and K_L is Langmuir constant related with affinity of the point of union (L.mg^{-1}). The value of Q_m is calculated from the slope ($1/Q_m$) and intercept ($1/Q_m$ b) using the linier plot of C_e/q_e versus C_e. The values of Q_m and K_L were obtained from Slope and intercept of the plots.

The Freundlich isotherm equation for the adsorption of phenol is calculated from linear parameter as following Eq. (4):

$$\log Q_e = \log K_F + \frac{1}{n} \log C_e \quad (4)$$

where the values of K_F and $1/n$ are the Freundlich constants which related to the adsorption capacity and adsorption intensity, respectively. Their values were calculated from the intercept ($log\ K_F$) and slop ($1/n$) based on the linier plot of log Q_e versus log C_e.

It is very important to obtain the appropriate correlation coefficient (R^2) for the adsorption equilibrium from the curve of Langmuir and Freundlich isotherm. Based on the data, both adsorption isotherms possess a fit linearity correlation coefficient $R^2 > 0.9$ that can be described as a favorable behavior. The comparison studies of the Langmuir and Freundlich adsorption of phenol onto the composites were shown in Figure 6 and in Table 2. In this study, the curve of Langmuir and Freundlich isotherms tends to fit equilibrium data with the excellent correlation coefficient ($R^2 > 0.91$). The Langmuir isotherms tend to show the favorable sorption with the presence of micropore or monolayer indicating chemisorption process. The Freundlich isotherm is widely used as indicative of mesopore with multilayer process relating with physisorption interaction within phenol molecules. However, the Langmuir equilibrium for the ZnO/AC-KOH composite showed a low value of correlation coefficient (R^2), while the Freundlich isotherm showed a good value of correlation coefficient (R^2). This phenomenon showed that the interaction of phenol tends to multilayer with physisorption process.

3.10 Adsorption Kinetic of Activated Carbon

Investigation of the kinetics from experimental data was carried from different contact times in the range of 15 to 60 min. The adsorption kinetic was evaluated using the pseudo-first-order and pseudo-second-order (Table 3) followed Eqs. (5) and (6), respectively [23,24].

Table 2. Isotherm constants and regression data for Langmuir and Freundlich for phenol removal using composites.

Composites	Langmuir			Freundlich		
	Q_m (mg.g^{-1})	K_L (L.mg^{-1})	R^2	K_F (mg.g^{-1})	n	R^2
ZnO/AC-KOH	15.55	0.64	0.778	2.40	1.822	0.912
ZnO/AC-$ZnCl_2$	1.55	−0.06	0.986	17.45	−1.989	0.967
ZnO/AC-H_3PO_4	1.07	−0.02	0.991	451.65	−0.884	0.992

Table 3. Pseudo-second-order parameters for the phenol removal onto different composites

Composites	Pseudo-second-order		
	k_2 (g.mg^{-1}.min^{-1})	q_e (mg.g^{-1})	R^2
ZnO/AC-KOH	0.73	2.43	0.871
ZnO/AC-$ZnCl_2$	0.03	3.33	0.987
ZnO/AC-H_3PO_4	0.03	3.17	0.972

$$\log\left(q_e - q_t\right) = \log q_e - \frac{k_1}{2.303}t \quad (5)$$

$$\frac{t}{q_t} = \frac{1}{k_2 q_e^2} + \frac{1}{q_t}t \quad (6)$$

where q_e and q_t are the amount of phenol adsorbed (mg.g^{-1}) at equilibrium and at t (min) time, k_1 is the pseudo-first-order equilibrium rate constant (min^{-1}) and k_2 is the pseudo-second-order rate constant (g.mg^{-1}.min^{-1}). Determination of constant (k_2) can be obtained from the plot t versus t/q_t relating to the values of q_e and the intercept.

Based on kinetic data, the pseudo-first-order for all composites showed very low value of correlation coefficient (R^2) which is indicative of the unfamiliar interaction through the physisorption process. However, the pseudo-second-order tends to fit equilibrium on better correlation coefficients (R^2) which is close to unity equilibrium as displayed in Figure 7. The correlation coefficient (R^2) values are 0.871, 0.987 and 0.972 for the ZnO/AC-KOH, ZnO/AC-$ZnCl_2$ and ZnO/AC-H_3PO_4, respectively. This result assumed that mechanism process of the removal of phenol onto composites occurred by the pseudo-second-order relating with the chemisorption process. This result is relevant with previous work that the presence of metal oxide such as zinc oxide on the surface gave contribution on the pore with varying size and enriched the oxygen functional groups. The phenol adsorption happened by ligand exchange/chemisorption through the attractive forces by sharing and exchanging of the electrons [25–27].

4. Conclusions

The composite was successfully prepared from oil palm shell activated carbon using different activating agents and modified with zinc oxide. Chemical activation has influenced the formation of pore structure. The highest BET surface area was obtained from activated carbon prepared by phosphoric acid. All adsorption desorption isotherm curves showed open hysteresis at low relative pressure as an indication of pore desorption process. The SEM micrograph of composites showed disorientation surface with irregular pore size structure. The isotherm adsorption of phenol onto composite followed the Langmuir and Freundlich models with good fit linearity (R^2>0.9) and the exception for the ZnO/AC-KOH with lower correlation coefficient (R^2). The kinetic model was favorable for the pseudo-second-order compared to the pseudo-first-order. The results of this study showed that ZnO/activated carbon composite is effective for removal of phenol from the aqueous solution.

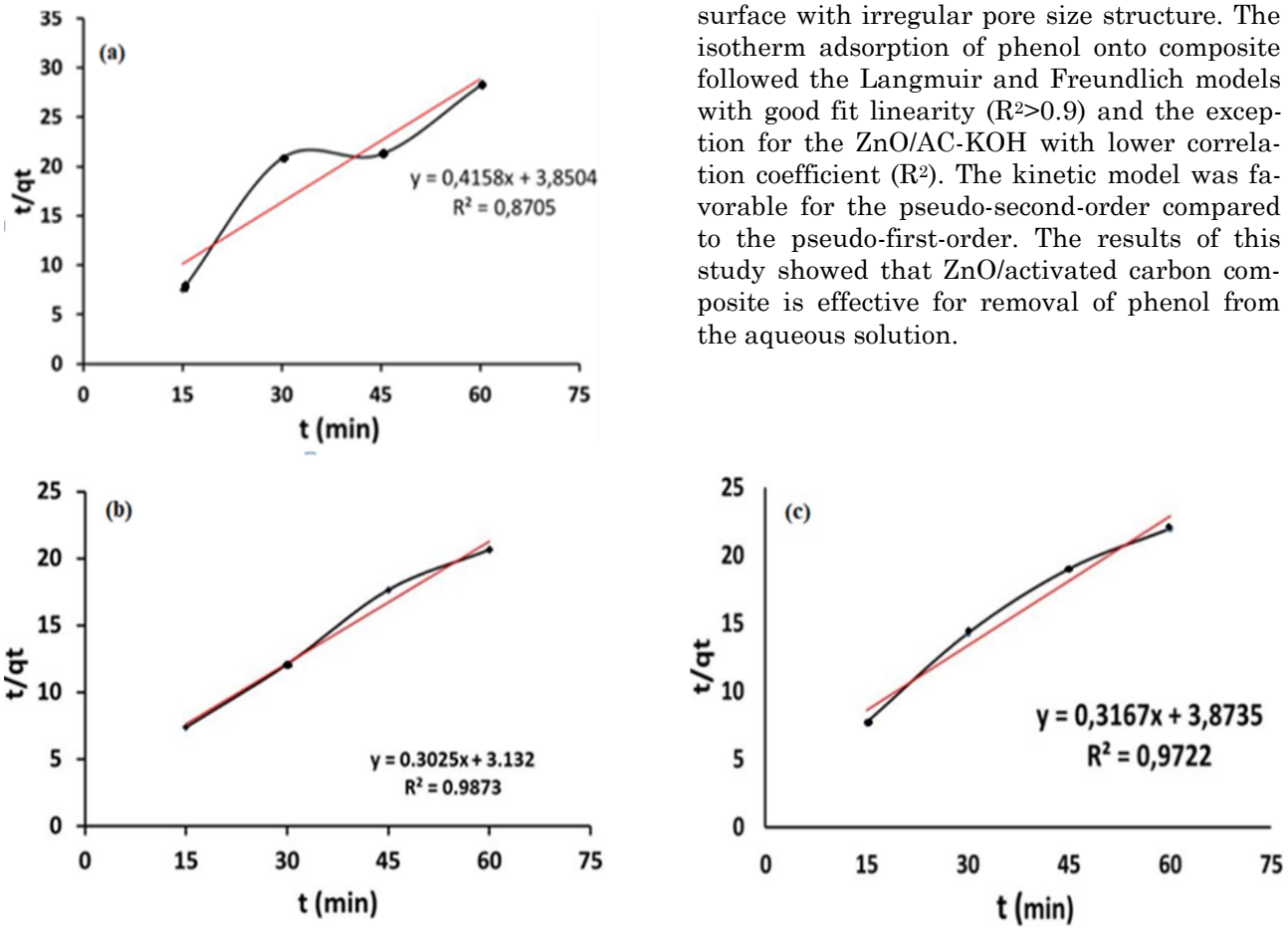

Figure 7. Kinetics of phenol adsorption based on the pseudo-second order (a) ZnO/AC-KOH; (b) ZnO/AC-$ZnCl_2$; (c) ZnO/AC-H_3PO_4.

Acknowledgments

The author would like to acknowledge the support to the Chemistry Department, Faculty Mathematics and Natural Sciences of Universitas Islam Indonesia and DPPM for funding this project with No: 11/Dir/DPPM/70/ Pen.unggulan/PIIII/XI/2018.

References

[1] Rodrigues, L.A., da Silva, M.L.C.P., Alvarez-Mendes, M.O., Coutinho, A.d.R., Thim, G.P. (2011). Phenol removal from aqueous solution by activated carbon produced from avocado kernel seeds. *Chemical Engineering Journal*, 174(1), 49–57, doi: 10.1016/j.cej.2011.08.027.

[2] Li, Y., Liu, X. (2014). Activated carbon/ZnO composites prepared using hydrochars as intermediate and their electrochemical performance in supercapacitor. *Materials Chemistry and Physics*, 148(1-2), 380–386, doi: 10.1016/j.matchemphys.2014.07.058.

[3] Hameed, B.H., Rahman, A.A. (2008). Removal of phenol from aqueous solutions by adsorption onto activated carbon prepared from biomass material. *Journal of Hazardous Materials*, 160(2-3), 576–581, doi: 10.1016/j.jhazmat.2008.03.028.

[4] Hasan, Z., Jhung, S.H. (2015). Removal of hazardous organics from water using metal-organic frameworks (MOFs): Plausible mechanisms for selective adsorptions. *Journal of Hazardous Materials*, 283, 329–339, doi: 10.1016/j.jhazmat.2014.09.046.

[5] Muthirulan, P., Meenakshisundararam, M., Kannan, N. (2013). Beneficial role of ZnO photocatalyst supported with porous activated carbon for the mineralization of alizarin cyanin green dye in aqueous solution. *Journal of Advanced Research*, 4, 479–484, doi: 10.1016/j.jare.2012.08.005.

[6] Cruz, G.J.F., Gómez, M.M., Solis, J.L., Rimaycuna, J., Solis, R.L., Cruz, J.F., Rathnayake, B., Keiski, R.L. (2018). Composites of ZnO nanoparticles and biomass based activated carbon: adsorption, photocatalytic and antibacterial capacities. *Water Science and Technology*, 2017(2), 492–508, doi: 10.2166/wst.2018.176.

[7] Lee, K.S., Park, C.W., Kim, J.D. (2018). Synthesis of ZnO/activated carbon with high surface area for supercapacitor electrodes. *Colloids and Surfaces A: Physicochemical and Engineering Aspects*, 555, 482–490, doi: 10.1016/j.colsurfa.2018.06.077.

[8] Xu, J., Chen, L., Qu, H., Jiao, Y., Xie, J. Xing, G. (2014). Preparation and characterization of activated carbon from reedy grass leaves by chemical activation with H_3PO_4. *Applied Surface Science*, 320, 674–680, doi: 10.1016/j.apsusc.2014.08.178.

[9] Cherik, D., Louhab, K. (2017). Preparation of microporous activated carbon from date stones by chemical activation using zinc chloride. *Energy Sources, Part A: Recovery, Utilization, and Environmental Effects*, 39(18), 1935–1941, doi: 10.1080/15567036.2017.1390012.

[10] Ahmaruzzaman, M, .Sharma, D.K. (2005). Adsorption of phenols from wastewater. *Journal of Colloid and Interface Science*, 287(1), 14–24, doi: 10.1016/j.jcis.2005.01.075.

[11] Allwar, A., Hartati, R., Fatimah, I. (2017). Effect of nitric acid treatment on activated carbon derived from oil palm shell. *AIP Conference Proceedings,* 1823, 020129, doi: 10.1063/1.4978202.

[12] Yakout, S.M., El-Deen, G.S. (2016). Characterization of activated carbon prepared by phosphoric acid activation of olive stones. *Arabian Journal of Chemistry*, 9, S1155–S1162, doi: 10.1016/j.arabjc.2011.12.002.

[13] Andas, J., Ab. Satar, N.A. (2018). Synthesis and Characterization of Tamarind Seed Activated Carbon using Different Types of Activating Agents: A Comparison Study. *Materials Today: Proceedings*, 5(9), 17611–17617, doi: 10.1016/j.matpr.2018.06.079.

[14] Dudzińska, A. (2014). Investigation of adsorption and desorption of acetylene on hard coal samples from Polish mines. *International Journal of Coal Geology*, 24(31), 128–129, doi: 10.1016/j.coal.2014.03.007.

[15] Yorgun, S., Yıldız, D. (2015). Preparation and characterization of activated carbons from Paulownia wood by chemical activation with H_3PO_4. *Journal of the Taiwan Institute of Chemical Engineers*, 53, 122–131, doi: 10.1016/j.jtice.2015.02.032.

[16] Selvakumar, M., Bhat, D.K., Aggarwal, A.M., Prahladh Iyer, S., Sravani, G. (2010). Nano ZnO-activated carbon composite electrodes for supercapacitors. *Physica B: Condensed Matter*, 405(9), 2286–2289, doi: 10.1016/j.physb.2010.02.028.

[17] Sasirekha, C., Arumugam, S., Muralidharan, G. (2018). Green synthesis of ZnO/carbon (ZnO/C) as an electrode material for symmetric supercapacitor devices. *Applied Surface Science*, 449, 521–527, doi: 10.1016/j.apsusc.2018.01.172.

[18] Mopoung, S., Jitchaijaroenkul, K. (2017). Characterization of Activated Carbon from Eggshell Membranes Prepared Using Sodium Acetate and Zinc Metal Activation. *American Journal of Applied Sciences*, 14(8), 737–747, doi: 10.3844/ajassp.2017.737.747.

[19] Bhadra, B.N., Ahmed, I., Jhung, S.H. (2016). Remarkable adsorbent for phenol removal from fuel: Functionalized metal–organic framework. *Fuel*, 174, 43–48, doi: 10.1016/j.fuel.2016.01.071.

[20] Zhang, Z., Niu, H., Fernández, Y., Menéndez, J.A., Peng, J., Zhang, Z., Zhang, L., Duan, X. (2010). Effect of temperature on the properties of ZnO/Activated carbon composites from spent catalysts containing zinc acetate. *Journal of the Taiwan Institute of Chemical Engineers*, 41(5), 617–621, doi: 10.1016/j.jtice.2009.12.004.

[21] Elkady, M., Hassan, H., Amer, W., Salama, E., Algarni, H., Shaaban, E. (2017). Novel Magnetic Zinc Oxide Nanotubes for Phenol Adsorption: Mechanism Modeling. *Materials*, 10(12), 1355, doi: 10.3390/ma10121355.

[22] Saleh, T.A., Alhooshani, K.R., Abdelbassit, M.S.A. (2015). Evaluation of AC/ZnO composite for sorption of dichloromethane, trichloromethane and carbon tetrachloride: kinetics and isotherms. *Journal of the Taiwan Institute of Chemical Engineers*, 55, 159–169, doi: https://doi.org/10.1016/j.jtice.2015.04.004.

[23] Ho, Y.S., McKay, G. (1998). Sorption of dye from aqueous solution by peat. *Chemical Engineering Journal*, 70(2), 115–124, doi: 10.1016/S0923-0467(98)00076-1.

[24] Kennedy, L.J., Vijaya, J.J., Kayalvizhi, K., Sekaran, G. (2007). Adsorption of phenol from aqueous solutions using mesoporous carbon prepared by two-stage process. *Chemical Engineering Journal*, 132(1-3), 279–287, doi: 10.1016/j.cej.2007.01.009.

[25] Aliakbarian, B., Casazza, A.A., Perego, P. (2015). Kinetic and Isothermal Modelling of the Adsorption of Compounds from Olive Mill Wastewater onto Activated Carbon. *Food Technology and Biotechnology*, 53(2), 207–214, doi: 10.17113/ftb.53.02.15.3790.

[26] Kumar, P.S., Korving, L., Keesman, K.J., van Loosdrecht, M.C.M., Witkamp, G.-J. (2016). Effect of pore size distribution and particle size of porous metal oxides on phosphate adsorption capacity and kinetics. *Chemical Engineering Journal*, 358, 160–169, doi: 10.1016/j.cej.2018.09.202.

[27] Simonin, J.-P. (2016). On the comparison of pseudo-first order and pseudo-second order rate laws in the modeling of adsorption kinetics. *Chemical Engineering Journal*, 300, 254–263, doi: 10.1016/j.cej.2016.04.079.

Selected and Revised Papers from 3rd International Conference on Chemistry, Chemical Process and Engineering 2020 (IC3PE 2020) (https://chemistry.uii.ac.id/ic3pe/) (Universitas Islam Indonesia (UII), Labuan Bajo, Nusa Tenggara Timur, Indonesia by 30th September – 1st October 2020) after Peer-reviewed by Scientific Committee of IC3PE 2020 and Peer-Reviewers of Bulletin of Chemical Reaction Engineering & Catalysis.
Editors: I. Istadi; Is Fatimah